

# Study on future European winged reusable launchers

*Steffen Callsen\*, Sven Stappert\*, Martin Sippel\**

*\*Institute of Space Systems, German Aerospace Center (DLR), Bremen Germany*

*Steffen.Callsen@dlr.de, Sven.Stappert@dlr.de, Martin.Sippel@dlr.de*

## Abstract

The realization of reusability for launch vehicles is expected to lower launch costs – subsequently enabling a thriving space industry. Therefore, several high-performance semi-reusable launch vehicle concepts are designed and investigated based on the premise of potential implementation into the Ariane program by using stage and engine parts from future Ariane 6 hardware. These vehicles are imagined as a combination of a winged reusable booster and one to two expendable upper stages for injection into a geostationary transfer orbit (GTO). First stage reusability is achieved by the “In-Air Capturing” method proposed by DLR which is currently studied in the H2020 project FALCon. A payload mass of approximately 14 tons into GTO is pursued, consequently surpassing the anticipated payload mass of the Ariane 64. This paper presents the current technical status of the different investigated RLV configurations including geometrical shape, layout, propellant system, propulsion, aerodynamics and structural layout. Additionally, the designs shall be critically analysed regarding their suitability and applicability for a potential implementation into the European launcher roadmap.

## Abbreviations

|        |   |      |                                |
|--------|---|------|--------------------------------|
| CFRP   | Carbon Fibre Reinforced Polymer   | LLPM | Lower Liquid Propulsion Module |
| CSG    | Centre Spatial Guyanais   | LOX  | Liquid Oxygen                  |
| FALCon | Formation flight for in-Air Launcher<br>1 <sup>st</sup> stage Capturing demonstration | MECO | Main Engine Cut-Off            |
| GLOM   | Gross Lift-Off Mass   | RLV  | Reusable Launch Vehicle        |
| GTO    | Geostationary Transfer Orbit  | SECO | Second Engine Cut-Off          |
| IAC    | In-Air-Capturing  | SI   | Structural Index               |
| LCH4   | Liquid Methane  | SLME | SpaceLiner Main Engine         |
| LEO    | Low Earth Orbit   | TPS  | Thermal Protection System      |
| LH2    | Liquid Hydrogen   | ULPM | Upper Liquid Propulsion Module |

## 1. Introduction

With Europe’s newest heavy-lift launch vehicle, the Ariane 6, inching closer to its maiden flight, talks and discussions are already taking place for a next generation vehicle. This is happening primarily due to the massively changing launcher market in the last few years which could put the Ariane 6 at an economic disadvantage in comparison to semi- or fully reusable launchers. Beyond the strategy of continuously improving and refining the Ariane 6 itself (examples for (potential) realization: ASTRIS kick stage [1], CFRP upper stage [2], liquid methalox boosters [1]), a mid-term strategy for European spaceflight needs to be developed. This could see the creation and development of a new generation of launchers enabling reusability of the lower stage, while still expanding on the performance as well as mission versatility. In light of potential European human spaceflight [1] as well as deep space exploration, a multipurpose high-performance launcher system is required beyond the Ariane 6.

This study aims to be a starting point for these discussions with the development of high-performing launcher systems based on different propulsion systems which are under development in Europe – both in active development as well as being at a concept stage. These include the full-flow staged combustion SpaceLiner Main Engine and the Prometheus engine in two versions with liquid methane or liquid hydrogen as fuel and liquid oxygen as oxidizer.

For this study, the recoverability method is focused on winged stages with double-delta wings. These re-enter on a gliding flightpath and are “captured in the air” by being actively captured by a waiting aircraft with a capturing device. Nevertheless, similar studies with vertical landing stages similar to SpaceX’s Falcon 9 are investigated in parallel [1]. A trade-off between these studies should be performed in the future.

## 2. Mission and Design Assumptions

In this chapter, the general layout of the mission and the design are presented. First, the general requirements are discussed, followed by a description of the different propulsion systems evaluated. Lastly, the recovery method “In-Air Capturing” for the first stage booster is presented.

### 2.1 Mission Requirements

In order to have a flexible and adaptable launch system available for commercial as well as institutional payloads, the launch systems are planned to be used flexibly with two or three stages respectively. Furthermore, expecting an increase in exploration missions beyond Earth orbit to Moon or Mars in the next decade, the targeted payload mass shall exceed the currently planned value of the Ariane 6 while still achieving reusability. Consequently, a GTO payload mass of 14 tons is targeted in a 3-stage configuration when being launched from CSG in Kourou, French Guiana. This also enables transportation of large payloads to the Moon and beyond. When serving customers in LEO, the 2-stage variant can deliver more than 25 tons to an orbit going to the International Space Station. However, such a mission is not shown in this paper.

### 2.2 Propulsion systems

Multiple different propulsion systems and their impact on the overall system performance are investigated in this study. For these 3-stage systems, the propulsion systems are varied across all options in the first and second stage – both on the engine cycle as well as the propellant type. The third stage is always powered by the hydrolox Vinci engine of the Ariane 6 upper stage (expander cycle), the technical data is shown in Table 1.

The first option to be investigated is the SpaceLiner Main Engine (SLME) [3], a full-flow staged combustion rocket motor concept fuelled by liquid oxygen and liquid hydrogen. It was originally envisioned for the DLR SpaceLiner hypersonic spacecraft concept for Earth Point-to-Point operations, which requires an efficient and high-performance engine. It is a powerful engine with thrust up to approximately 2.4 MN which is comparable to SpaceX’s Raptor and Blue Origin’s BE-4 engine. The latest work performed on the SLME is component analysis of the turbomachinery and pre-burners in cooperation with *SoftInWay* [4]. The technical data of the SLME and Vinci engine is shown in Table 1.

Table 1: Technical data of the SpaceLiner Main Engine and Vinci [3, 5]

|                                   | SLME RLV<br>Booster | SLME 2 <sup>nd</sup><br>ELV stage | Vinci |
|-----------------------------------|---------------------|-----------------------------------|-------|
| Mixture ratio [-]                 | 6.5                 | 5.5                               | 5.8   |
| Chamber pressure [MPa]            | 16.9                | 15.1                              | 6.1   |
| Mass flow [kg/s]                  | 555                 | 481                               | 39    |
| Expansion ratio [-]               | 33                  | 59                                | 175   |
| Specific impulse in vacuum [s]    | 435                 | 451                               | 457   |
| Specific impulse at sea level [s] | 390                 | 357                               | -     |
| Thrust in vacuum [kN]             | 2356                | 2116                              | 174.8 |
| Thrust at sea level [kN]          | 2111                | 1678                              | -     |

In Europe, the currently ongoing engine development is mainly focused on the Prometheus engine [6]. It is a 1 MN class engine fuelled by liquid oxygen and liquid methane. The turbomachinery layout is based on a classic gas generator open cycle, which enables a mono-shaft turbopump for both propellants. It is planned to use additive manufacturing processes to lower the cost and simplify production.

Additionally, there has been an interest in developing a version with hydrogen instead of methane, called the Prometheus-H or a future Vulcain variant. The aim of such a program would be to reduce the cost of the Vulcain by applying the cost advantages of the Prometheus program like additive manufacturing. Hydrogen would greatly increase the efficiency due to a higher specific impulse, but comes at the disadvantage of more challenging propellant and thermal operations. This engine variant would require a dual-shaft turbopump but its overall design can be similar.

As the Prometheus is still in development and the Prometheus-H only a theoretical concept at this point in time, the data shown in Table 2 is calculated based on in-house assessments. At last, it should be remarked that for the second stages an expansion ratio of 59 is low, enabling the vacuum optimized SLME version to also be operated at sea level conditions as is necessary for the SpaceLiner. As this is not an operational requirement for these vehicles, future studies could investigate optimizing the 2<sup>nd</sup> stage engines by increasing the size of the nozzle and thereby the expansion ratio.

Table 2: Calculated technical data of the Prometheus and Prometheus-H engines

|                                   | <b>Prometheus<br/>RLV Booster</b> | <b>Prometheus<br/>2<sup>nd</sup> ELV stage</b> | <b>Prometheus-H<br/>RLV Booster</b> | <b>Prometheus-H<br/>2<sup>nd</sup> ELV stage</b> |
|-----------------------------------|-----------------------------------|--|-------------------------------------|--|
| Mixture ratio [-]                 | 2.68                              | 2.68   | 6.0                                 | 6.0  |
| Chamber pressure [MPa]            | 12                                | 12   | 12                                  | 12   |
| Mass flow [kg/s]                  | 422.5                             | 422.5  | 325                                 | 325  |
| Expansion ratio [-]               | 20                                | 59   | 20                                  | 59   |
| Specific impulse in vacuum [s]    | 319                               | 337  | 405                                 | 431  |
| Specific impulse at sea level [s] | 287                               | 251  | 365                                 | 317  |
| Thrust in vacuum [kN]             | 1322                              | 1397   | 1292                                | 1375   |
| Thrust at sea level [kN]          | 1190                              | 1040   | 1164                                | 1011   |

### 2.3 Recovery method

In order to recover the first stage, it will be equipped with wings allowing the stage to decelerate significantly by using atmospheric drag. While re-entering, a high angle of attack will be maintained as long as possible to use the higher and less dense part of the atmosphere to decelerate. Later, the angle of attack is reduced to avoid high lateral loads. Here, first stage separation velocities of not more than 2.5 km/s are targeted in order to limit the re-entry loads. Within the design space of these combinations, the density of the propellants and consequently size of the vehicle as well as the mass distribution along the winged stage play a crucial role in the determination of a stable re-entry performance from hypersonic down to subsonic velocities. Once the stage is flying below the speed of sound, which occurs at approximately 15-20 km altitude, it glides at a relatively shallow angle towards the ground, comparable to the final mission profile of the Space Shuttle Orbiter.

The recovery is performed below an altitude of 10 km with a method called “in-air-capturing” (IAC) which is patented by DLR [7]. It uses an airplane of sufficient size to fly in formation with the stage and capture it during its glide to the ground. Therefore, it is equipped with an aerodynamically controlled capturing device (ACCD) at the end of a long rope, which is able to match the RLV stage’s exact position by being actively controlled. Once the RLV stage is connected to the airplane, it is towed back to the launch site before it is released for an autonomous, unpropelled landing on a runway. Figure 1 displays the in-air-capturing methodology from launch to landing.

The key advantage of the in-air-capturing method is the non-usage of additional propellant to decelerate the stage. However, the addition of wings increases the overall inert mass and adds complexity to the system, for example in the aerodynamics, structure and thermal protection system.

The capturing is currently being investigated and tested on a laboratory scale within the EC funded project FALCon [8, 9], which is led by DLR in cooperation with other European partners. Besides full-scale simulations, two autonomous test vehicles will be flown in order to test the capturing in the near future. The technology shall have a TRL beyond 4 after the end of the project. Results are already available and published in [10, 11, 12, 13, 14, 15].

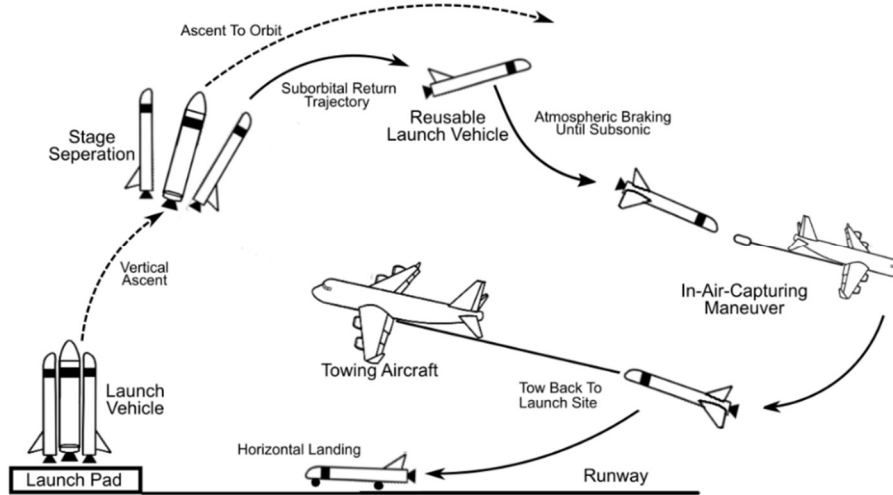


Figure 1: Mission profile of the proposed in-air-capturing method

### 2.4 Mission Profile

In a 3-stage configuration, the large second stage requires a specific mission profile to ensure splashdown in an open Ocean area far away from any populated areas (see Figure 2). Because it is able to achieve orbital velocities on its own, the stack is injected into an intermediate orbit with a low perigee of around 35 km. This ensures that the second stage enters the atmosphere about half an orbit later which places its re-entry area in the Pacific Ocean. The third stage accelerates the payload to the target orbit. In case of a 2-stage mission to LEO, the second stage needs to perform a dedicated re-entry manoeuvre upon separation until the in-air-capturing is successfully performed. The first stage performs its re-entry manoeuvre upon separation until the in-air-capturing is successfully performed.

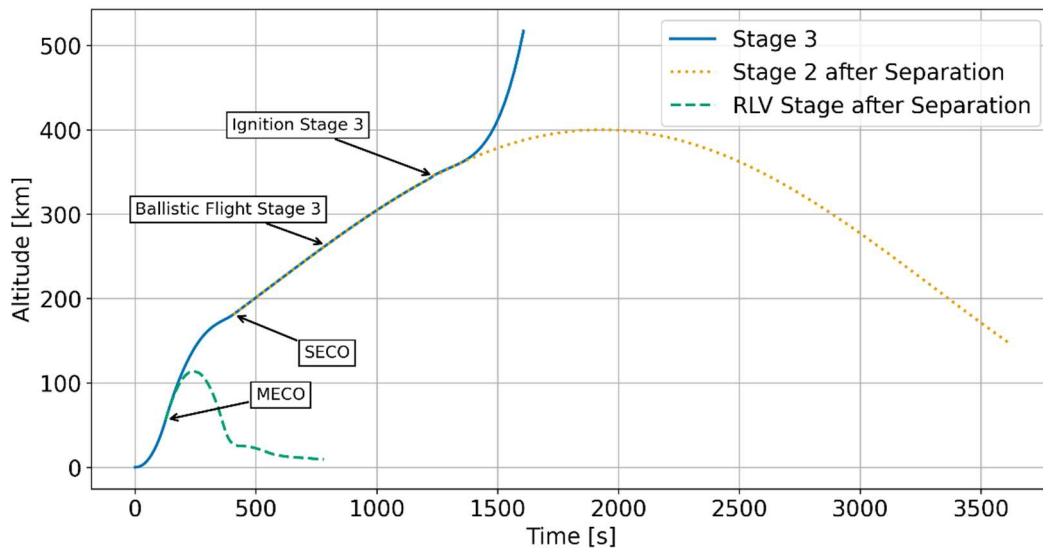


Figure 2: Exemplary mission profile to GTO

### 3. Vehicle design and analysis

This chapter contains a description of all the different launcher versions that are created and analysed thoroughly. Two variants with full-flow staged combustion engines are designed which differ mainly in the design of the wings and the aerodynamic performance. Because of the versatility of the gas-generator engine, multiple designs are analysed: A pure LOX-hydrogen version, a pure LOX-methane version as well as a hybrid version combining a LOX-methane RLV-stage and a LOX-hydrogen expendable second stage. The RLV stage is placed in a parallel configuration to the rest of the vehicle consisting of the second and third stage as well as the payload and fairing.

### 3.1 Version B-flexible: Staged combustion, flexible wing

Version B is the baseline version for this study as well as for others. For example, it is used in the Horizon 2020 project FALCon as a reference stage to investigate the in-air-capturing recovery methodology when flying in formation with the aircraft and attaching to the aerodynamically controlled capturing device. The versions described in the subsequent sections are mainly differing in the first two stages.

Version B uses liquid hydrogen and liquid oxygen in all three stages. The first two stages are powered by the staged combustion engine SLME – four in the RLV stage and one vacuum optimized engine in the second stage (compare Table 1). The Vinci engine injects the third stage as well as the payload into the final orbit.

370 tons of propellant are accommodated in the 60-meter-long and 5.4-meter wide stage (see Figure 3). If the wing is fully deployed, the vehicle has a wing span of about 37 meters which enables a trimmed subsonic lift-to-drag ratio of approximately 6 which is needed to allow a shallow glide path during the In-Air-Capturing procedure, thus facilitating the matching of glide path and velocity by the towing aircraft. When extended, it is a double delta wing with the outer part increasing the aspect ratio and therefore enabling the high lift-to-drag ratios in the subsonic range.

This version features foldable wings. The advantage of such a design is related to reduced flow perturbances during ascent and avoiding interaction between the nose shock and the wing's leading-edge shock, otherwise resulting in potentially critical heat flux values. These in turn demand for a reinforced thermal protection system (TPS) at the affected wing parts. This phenomenon was discussed in several DLR studies and was identified as being more critical, the higher the re-entry velocity [16, 17, 18]. Hence, with retractable wings the effective span during re-entry could be limited to make sure that the wings are not lying within the shock-shock interaction. When transitioning to subsonic speed, the wing could be extended to allow for a higher lift-to-drag ratio, if adequately designed better than a fixed-wing configuration. From a mass standpoint, the mechanical folding system has not been adequately investigated yet, making it a huge critical aspect as its mass could be higher than is anticipated.

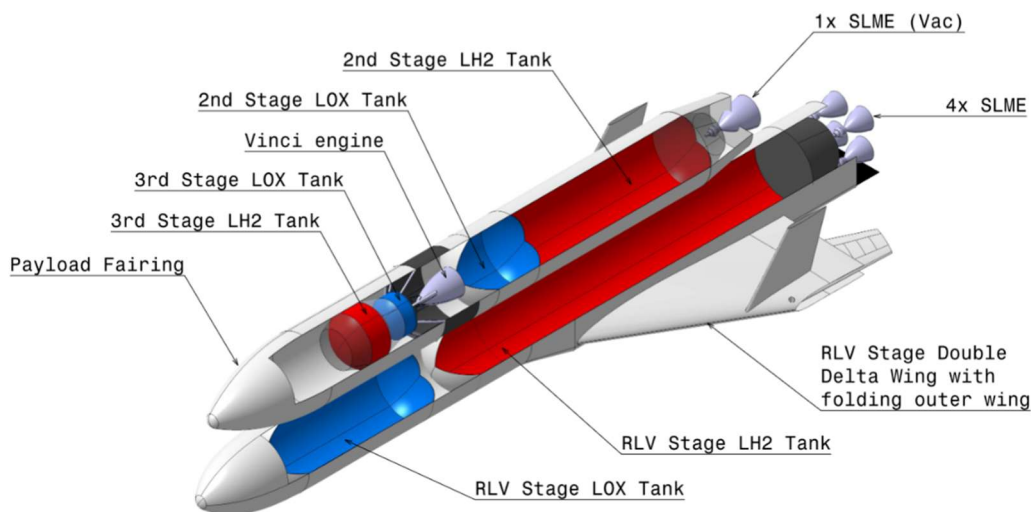


Figure 3: Version B architecture with a flexible wing in the 3-stage configuration

The second stage is designed closely to the Ariane 6 LLPM with a propellant loading of 150 tons and a diameter of 5.4 meters. Instead of the Vulcain 2.1 engine, it is also powered by the SLME engine which produces almost double the thrust leading to high accelerations of over 1 g directly after ignition and more than 5 g at the end of its flight. Due to its high thrust, the second stage burn is rather short at just over 5 minutes.

Because of the powerful second stage, the size of the third stage is reduced to a propellant loading of about 14 tons. In order to optimize the tank design and structural mass, the third stage's diameter is decreased to 4.0 meter and is moved under the fairing. The high efficiency of the Vinci engine enables the B-version to deliver almost 14 tons to a standard GTO orbit. The third stage is not changed significantly in the versions described below which is why it is not mentioned any further.

### **3.2 Version B-fixed: Staged combustion, fixed wing**

This variant of the B-version only differs marginally from the one described in the previous section. The primary change is in the wing with a fixed structure instead of a flexible. Due to some minor design changes, such as changing the surface area of the vertical fins, the mass between both stages differs slightly. However, the folding wing stage would have to account for a mechanical wing folding system of which no mass estimation was performed up to date. Determining this mass is a topic of future work and investigations have already started at DLR. However, this reduction in mass of about 1.8 tons does not lead to a substantial payload mass increase. Thus, it reduces the complexity of the mechanical system in the wings but does require more investigations regarding the potential impact of shock-shock interactions in the hypersonic range. This also applies to all following versions featuring a fixed wing structure.

### **3.3 Version G: Hydrogen gas generator, fixed wing**

Version G is the first gas generator version in this study. Instead of relying on the conceptual engine SLME, which would require a full development cycle and is still in the early phases of its design, the currently developed Prometheus is used for these analysis. In this first version, the adapted, hypothesized hydrogen version is installed, while in the following sections the actively developed methane version is used.

Because of the lower performance of the open gas generator cycle, the first stage requires more propellant than the B-version. Furthermore, because the propellant loading on the second stage is kept almost constant (only a change of 2 additional tons), the first stage's cut-off velocity needs to be higher (about 2.3 km/s) leading to even more propellant demand. Consequently, about 450 tons of propellant are filled into the tanks of version G. Due to this increase of over 20 percent, the diameter of the first stage is enlarged to 6.0 m so as to avoid having a long and thin stage.

Because of the lower thrust of the Prometheus-H in comparison to the SLME, the number of engines in the RLV stage is increased to 10 in total allowing for a thrust-to-weight ratio of more than 1.5 at lift-off, which is quite high and could be reduced in the future with one fewer engine. A single Prometheus-H engine with a vacuum optimized nozzle is used in the second stage. As its thrust is substantially lower than the SLME used in the B-version, its thrust-to-weight ratio is lower with about 0.7 g at ignition, increasing to 2.7 g at engine cut-off. As a consequence, the second stage burn is a lot longer at close to 8 minutes.

### **3.4 Version MH: Hybrid gas generator, fixed wing**

As a first step towards a fully methalox system, a hybrid version is created. It features the same hydrolox second stage as the version G, but uses the methalox Prometheus gas generator engine in the first stage. This leads to some design changes of the RLV stage. Due to the lower specific impulse of methane, a higher propellant loading of 620 tons is required. With a similar thrust magnitude than the Prometheus-H, the number of engines is increased to 11 leading to a thrust-to-weight ratio of about 1.45 at lift-off.

While having more propellant, the higher density of liquid methane leads to an overall reduction in size for the MH version. With a chosen diameter of 5.4 meters, the RLV stage is about 55 meters (with bodyflap), which is 10 meters shorter than version G. The second stage is kept the same as for the version G.

### **3.5 Version MM: Methane gas generator, fixed wing**

This last version shows the impact on the design if both stages feature the methalox Prometheus engine while still keeping the hydrolox 14-ton third stage with the Vinci engine. In order to have a similar TPS setup than the other gas generator versions, the cut-off velocity of the MM version is kept at about 2.3 km/s. As a consequence, the RLV stage needs 800 tons of propellant while the second stage requires 230 tons. This change increases the overall take-off mass substantially.

15 Prometheus engines are placed on the first stage to enable lift-off with a thrust-to-weight ratio of about 1.5. This high number of engines adds more complexity to the system, but also moves the center of mass further towards the rear of the vehicle leading to challenges in the aerodynamic design, which will be discussed in the subsequent section. The length of the vehicle only increases slightly by a couple of meters. However, the diameter is increased to 6.0 meters again to allow for the grown propellant loading.

While the second stage shrinks in size due to the higher density of methane, it is significantly heavier than the hydrolox stage in the previous versions. Consequently, a second engine needs to be installed (similar to some versions of the Centaur upper stage [19]) to enable a thrust-to-weight ratio at ignition of about 1 g. If only a single engine were used, the stage would not have sufficient thrust to lift the stack into the transfer orbit. However, because of the higher mass flow of the methalox Prometheus, this results in a fairly short burn of about 4.5 minutes with a peak acceleration of 5.1 g.

### 3.6 Analysis of the stages

As described in the previous sections, the launcher systems investigated in this study vary primarily in their propellants and propulsion system. However, these parameters have a significant impact on the overall system design. These impacts are described and analyzed in the following section. First, the size and mass estimations are compared both on stage as well as on system level. Second, the flight profile of the RLV stage is analyzed during the ascent and descent. Finally, a general assessment of the system's suitability to a European RLV roadmap is made.

Table 3 lists the estimated dimensions of the stages. The third stage is kept at the same size over all versions. It is placed under the fairing with a diameter of 4.0 meters and an overall length of 6.5 meters. As potential payloads could require significantly more space than is available, a longer fairing or interstage should be investigated. The second stage is approximately the same for the first four versions. With a diameter of 5.4 meters, they are resembling current Ariane state-of-the-art. Because of a slightly higher propellant mass in the gas generator versions and a different engine, the latter two are slightly longer. In contrast, the methane version is substantially smaller due to its higher density propellant while still carrying about 80 tons more.

In general, the fuselages of the RLV stages are relatively similar and only differ by about 10 meters in length. The primary volumetric enlargement is created by widening the G- and MM-stages from 5.4 to 6.0 meters. Thus, as an example, the MH-version's volume is more than 30 percent smaller in comparison to the G-version due to it having a 5.4 m diameter and being on the lower end of the length variation.

Table 3: Launcher size estimations by stage

|                                | <b>Version B<br/>LH<sub>2</sub>-SC,<br/>flexible</b> | <b>Version B<br/>LH<sub>2</sub>-SC,<br/>fixed</b> | <b>Version G<br/>LH<sub>2</sub>-GG</b> | <b>Version MH<br/>Hybrid-GG</b> | <b>Version MM<br/>LCH<sub>4</sub>-GG</b> |
|--------------------------------|--|---|--|---------------------------------|--|
| <b>Stage 1</b>                 | H370   | H370  | H450                                   | C620                            | C800                                     |
| Total length (incl. bodyflap)  | 59.1 m   | 59.1 m  | 64.5 m                                 | 54.5 m                          | 56.3 m                                   |
| Fuselage diameter              | 5.4 m  | 5.4 m   | 6.0 m                                  | 5.4 m                           | 6.0 m                                    |
| Total span                     | 36.9 m   | 36.9 m  | 35.5 m                                 | 34.9 m                          | 35.5 m                                   |
| <b>Stage 2</b>                 | H150   | H150  | H152                                   | H152                            | C230                                     |
| Total length (incl. fairing)   | 46.5 m   | 46.5 m  | 50.8 m                                 | 50.8 m                          | 41.5 m                                   |
| Fuselage diameter              | 5.4 m  | 5.4 m   | 5.4 m                                  | 5.4 m                           | 5.4 m                                    |
| <b>Stage 3 (under fairing)</b> | H14  | H14   | H14                                    | H14                             | H14                                      |
| Total length                   | 6.5 m  | 6.5 m   | 6.5 m                                  | 6.5 m                           | 6.5 m                                    |
| Fuselage diameter              | 4.0 m  | 4.0 m   | 4.0 m                                  | 4.0 m                           | 4.0 m                                    |

A general comparison of all vehicle's profiles as well as the Ariane 64 can be seen in Figure 4. Overall, they look similar in size to the Ariane 6 but have an additional stack for the second and third stage plus the payload. So, in fact, the launchers studied here are significantly larger but offer recovery and reusability of the first stage plus an additional 2.5 tons of GTO payload [20].

Having a larger and therefore heavier stage, the wing area necessary to enable a sufficient trimmed glide ratio for IAC is also higher. For the G-version, the wing area is about 420 m<sup>2</sup> at a maximum span of 35.5 m, an increase of about 60

percent in terms of wing area compared to the version B's 265 m<sup>2</sup>. In contrast, the MH and MM-version only require 350 m<sup>2</sup> and 400 m<sup>2</sup> respectively.

One major difference between the wings along all four versions is its positioning. A trade-off must be made between pitch stability in the hypersonic range and trimmed lift-to-drag ratio in the subsonic range. On the one hand, the hypersonic pitch stability benefits by having the hypersonic pressure point further behind the center of mass. On the other hand, the trimmed glide ratio benefits when having the subsonic pressure point and center of mass closer together.

The predominant influence on the center of mass is the mass of the engines, which increases from left to right in Figure 4. Therefore, the wing must be moved towards the back accordingly. The trailing edge of the two hydrogen versions is a few meters in front of the end of the fuselage. For the MH-version, the trailing edge is at the end of the fuselage and does not require any changes. In contrast, the large number of engines on the MM-version lead to a significant change of the center of mass requiring the trailing edge of the wing to be swept back in order to move the pressure point backwards. In this case, only the inner part of the wing is swept back while the outer trailing edge is kept constant.

The analysis and design of the wing needs to be further investigated in the future for better optimization for the use case. One example of this being already done is in another study related to the flight dynamics of such a winged stage including an analysis of the lateral direction stability [21]. Furthermore, more research regarding the criticality of potential shock-shock interactions and how this impacts the overall design need to be made.

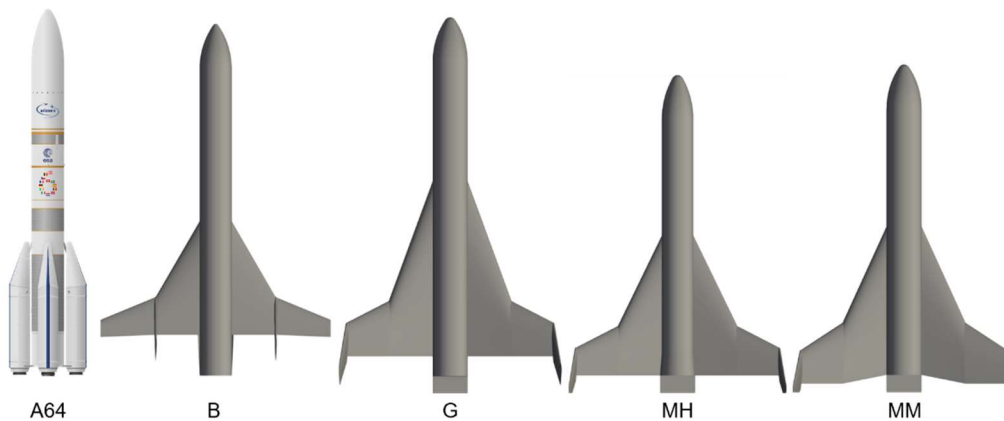


Figure 4: Comparison of all RLV stages with the Ariane 64 [22]

A detailed mass estimation breakdown for all versions is listed in Table 4, including margins for all elements. The structural index (SI) shown for each stage is calculated based on the dry mass and the propellant mass (see equation 1) and is a parameter for the overall structural efficiency.

$$SI = \frac{m_{\text{dry}}}{m_{\text{prop}}} \quad (1)$$

The first stage's dry masses differ by about 25 tons. The B-version defines the lower end of the spectrum with about 80 tons mainly due to its small size leading to an equally small structural mass. While each of the staged combustion engines are comparably heavy, having only four of them reduces the propulsion mass in total. In contrast, the MM-version both has the highest structural mass as well as the highest propulsion mass topping out at an overall dry mass of 105 tons. The relatively small MH version only has a dry mass of 85 tons, an increase of 5 tons over the B-version, while the version G is placed in the middle of the range with 95 tons. The hydrolox stages have significantly lower propellant masses which is why their structural index is high at about 20 percent. In contrast, the methalox stages are at about 13 percent.

The hydrolox second stages are very similar to each other, the main change is in the propulsion system. The gas generator Prometheus-H is estimated to be more than 1 ton lighter than its staged combustion counterpart. Only the methalox version differs significantly as it has approximately the same structural mass but holds 80 tons more propellant reducing the structural index from 12-13 percent to about 8 percent.

The third stage is very similar for all versions and mainly differ by small variations in their propellant loading. Therefore, the structural index is about 26-27 percent for all of them, which includes the SYLDA adapter for launcher two large payloads. Thus, for one large payload, the performance would be even higher.



Table 4: Launcher mass estimations by stage including margins

|                                      | <b>Version B<br/>LH<sub>2</sub>-SC,<br/>flexible</b> | <b>Version B<br/>LH<sub>2</sub>-SC,<br/>fixed</b> | <b>Version G<br/>LH<sub>2</sub>-GG</b> | <b>Version MH<br/>Hybrid-GG</b> | <b>Version MM<br/>LCH<sub>4</sub>-GG</b> |
|--------------------------------------|--|---|--|---------------------------------|--|
| <b>Stage 1</b>                       | H370   | H370  | H450                                   | C620                            | C800                                     |
| Structure incl. wings                | 47.2 t   | 45.4 t  | 59.3 t                                 | 49.4 t                          | 61.0 t                                   |
| Subsystems                           | 9.1 t  | 9.1 t   | 10.5 t                                 | 8.7 t                           | 11.0 t                                   |
| Propulsion                           | 16.2 t   | 16.2 t  | 18.1 t                                 | 19.9 t                          | 26.6 t                                   |
| Thermal                              | 8.1 t  | 8.1 t   | 7.2 t                                  | 6.5 t                           | 6.8 t                                    |
| Dry mass                             | 80.6 t   | 78.8 t  | 95.1 t                                 | 84.5 t                          | 105.4 t                                  |
| Ascent propellant reserves/residuals | plus 378.2 t   | 378.2 t   | 456.8 t                                | 628.2 t                         | 810.2 t                                  |
| GLOM                                 | 458.8 t  | 457.0 t   | 551.9 t                                | 712.7 t                         | 915.6 t                                  |
| Structural index                     | 21.3 %   | 20.8 %  | 20.8 %                                 | 13.5 %                          | 13.0 %                                   |
| <b>Stage 2</b>                       | H150   | H150  | H152                                   | H152                            | C230                                     |
| Structure incl. fairing              | 14.0 t   | 14.0 t  | 14.0 t                                 | 14.0 t                          | 13.2 t                                   |
| Subsystems                           | 1.0 t  | 1.0 t   | 0.9 t                                  | 1.0 t                           | 1.0 t                                    |
| Propulsion                           | 4.6 t  | 4.6 t   | 3.2 t                                  | 3.2 t                           | 4.4 t                                    |
| Thermal                              | 1.0 t  | 1.0 t   | 1.0 t                                  | 1.0 t                           | 0.7 t                                    |
| Dry mass                             | 20.6 t   | 20.6 t  | 19.1 t                                 | 19.1 t                          | 19.3 t                                   |
| Ascent propellant reserves/residuals | plus 153.6 t   | 153.6 t   | 155.6 t                                | 155.6 t                         | 234.8 t                                  |
| GLOM                                 | 174.2 t  | 174.2 t   | 174.7 t                                | 174.7 t                         | 254.1 t                                  |
| Structural index incl. fairing       | 13.4 %   | 13.4 %  | 12.3 %                                 | 12.3 %                          | 8.2 %                                    |
| <b>Stage 3 (under fairing)</b>       | H14  | H14   | H14                                    | H14                             | H14                                      |
| Structure incl. SYLDA                | 2.3 t  | 2.3 t   | 2.1 t                                  | 2.1 t                           | 2.1 t                                    |
| Subsystems                           | 0.8 t  | 0.8 t   | 0.8 t                                  | 0.8 t                           | 0.8 t                                    |
| Propulsion                           | 0.9 t  | 0.9 t   | 0.9 t                                  | 0.9 t                           | 0.9 t                                    |
| Thermal                              | 0.2 t  | 0.2 t   | 0.2 t                                  | 0.2 t                           | 0.2 t                                    |
| Dry mass                             | 4.2 t  | 4.2 t   | 4.0 t                                  | 4.0 t                           | 4.0 t                                    |
| Ascent propellant reserves/residuals | plus 15.6 t  | 15.7 t  | 15.4 t                                 | 15.4 t                          | 15.5 t                                   |
| GLOM                                 | 19.8 t   | 19.9 t  | 19.4 t                                 | 19.4 t                          | 19.5 t                                   |
| Structural index incl. SYLDA         | 26.9 %   | 26.8 %  | 26.0 %                                 | 26.0 %                          | 25.8 %                                   |
| <b>Vehicle</b>                       |  |   |  |                                 |  |
| GLOM                                 | 666.7 t  | 665.0 t   | 760.1 t                                | 920.8 t                         | 1203.2 t                                 |
| Payload                              | 13.9 t   | 13.9 t  | 14.1 t                                 | 14.0 t                          | 14.0 t                                   |

A graphical comparison of the overall data is shown in Figure 5. As indicated before, in terms of mass the B-version has the advantage of using the combination of liquid oxygen and liquid hydrogen with a highly efficient full-flow staged combustion engine. As a consequence, it has the lowest lift-off mass of all versions with about 670 tons. Changing the engine cycle to a gas generator but keeping hydrolox increases the lift-off mass by about 14 percent to 760 tons. Changing only the first stage to a methalox gas generator engine leads to an increase of about 21 percent in comparison to the version G and 38 percent to the baseline B-version, totaling about 920 tons. The largest increase in mass is viewable for the version MM as it has a methalox gas generator engine in the first and second stage. With about 1200 tons, it is an increase of 31 percent over the next in line version MH and 81 percent in comparison to the baseline. This is the primary reason why the MM version requires 15 Prometheus engines in the first stage to still manage to lift-off.

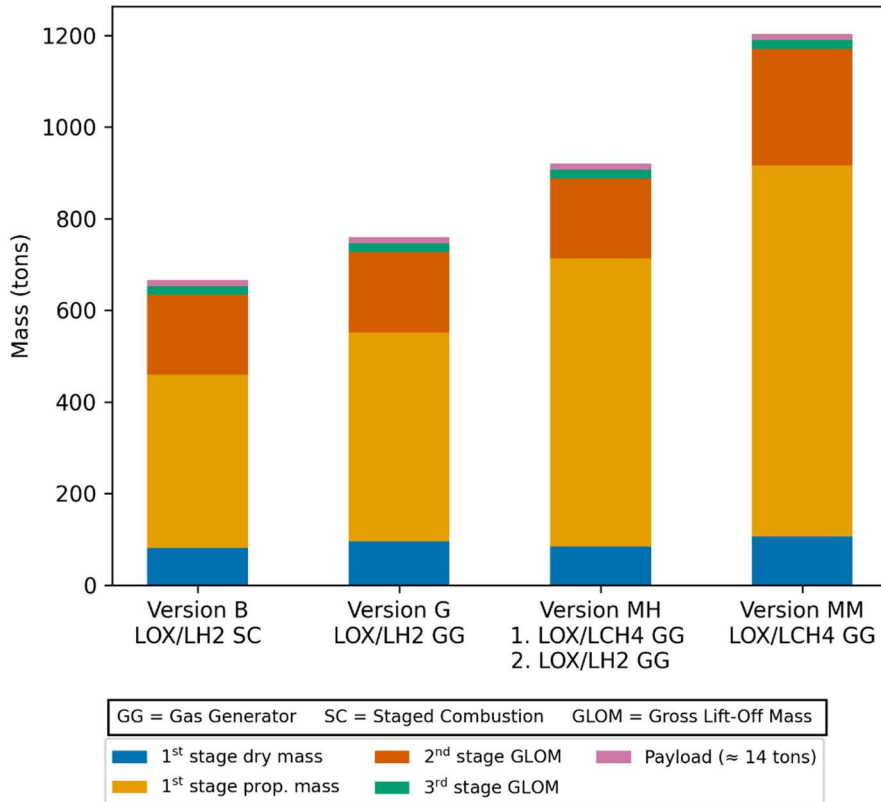


Figure 5: Mass comparison of RLV-types

Due to their differences in the propulsion system, the trajectories of the RLV stage are varying as well. First, the ascent until main engine cut-off is analysed, followed by the whole flight of the RLV from lift-off, over a ballistic coasting phase until the re-entry and glide towards Earth.

The graphs in Figure 6 show the ascent phase. In general, the biggest difference can be identified between the B-version and all others, marking the change in propulsion flow cycles. The B-version has a lower cut-off velocity of approximately 1.9 km/s, while having a flight time 30-40 seconds longer. Consequently, the acceleration profile is more benign topping out at about 3.3 g whereas the others rise to 4-5 g without any throttling. While a lower acceleration profile increases the gravity losses experienced by the B-version RLV stage, the highly efficient engine is able to counter this. On the positive side, a lower velocity eases the structural as well as the thermal loads on the vehicle, which can be seen in the dynamic pressure profile during the ascent but is also pronounced during the re-entry (see further below). All other versions separate at a velocity of about 2.3 km/s.

Both hydrogen versions have a higher cut-off altitude at about 65 km than their methane counterparts, which shut off their engines at a relatively low altitude of about 55 km. At this point in the flight, the dynamic pressure is still at approximately 1.3 and 1.5 kPa for the MH and MM-version respectively, which might lead to problems with the stage separation. This aspect needs to be further investigated in future studies.

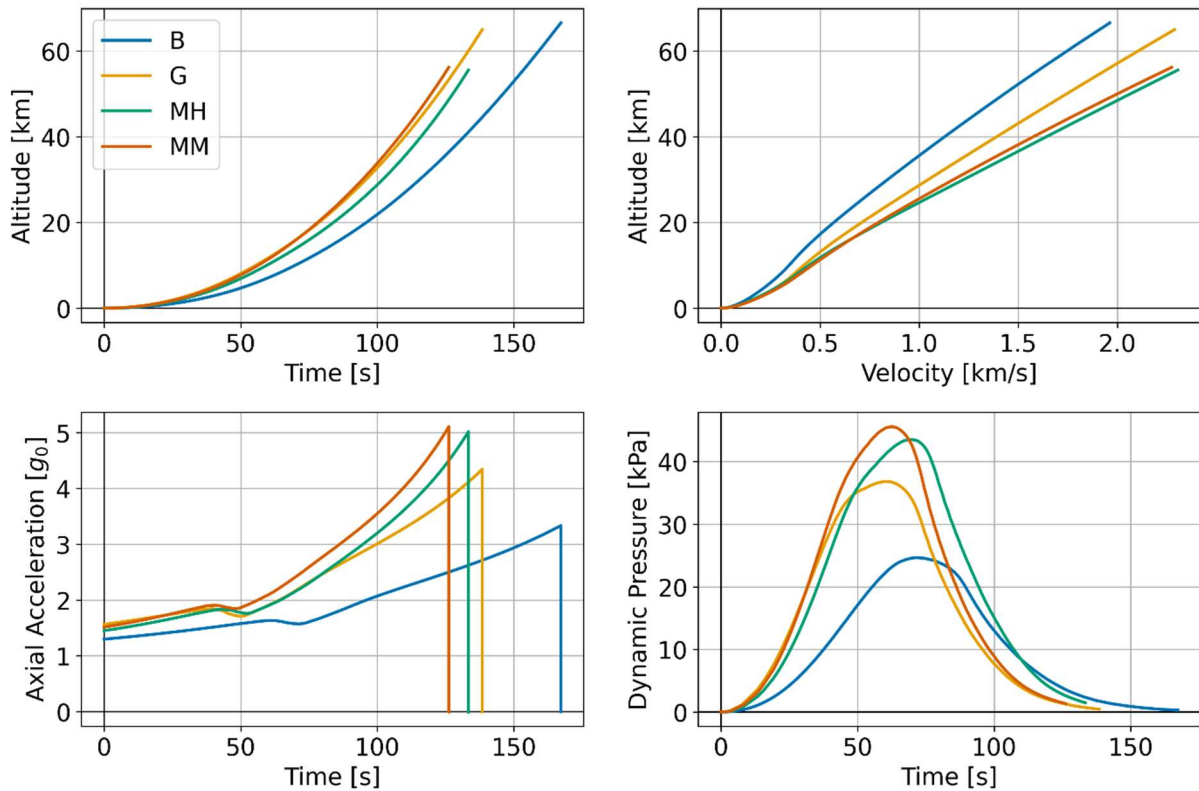


Figure 6: Comparison of the RLV stage's ascent profile

In Figure 7, the descent part of the winged stages flight is added to the diagrams. Furthermore, the axial acceleration profile is switched with the stagnation point heat flux which is more relevant for the descent.

After the ascent, all vehicles follow a ballistic trajectory peaking between 105 and 125 km. The version G achieves the highest altitude due to its high separation velocity as well as altitude. While the B-version also separates at a similar altitude, its lower velocity reduces the peak altitude to about 105 km. Both methane versions peak at approximately 115 km. Decreasing the altitude again, the vehicles re-enter the atmosphere and start creating both lift and drag below 50 km, with significant lift being created below 30 km.

All versions use their lifting capabilities to have a short phase with barely any vertical changes between 25 and 30 km allowing them to reduce their kinetic energy in the higher atmosphere and thereby reducing the maximum heat flux and dynamic pressure. During this phase, the lateral loads are capped to 3.5 g in order to minimize the structural loads on the vehicle and especially the wing. After the horizontal phase, the vehicles descend into a relatively constant glide until the simulation is cut-off at about 10 km in altitude. The glide ratio is slightly worse in the beginning because all vehicles perform a 180 degree turn with bank angles up to 40 degrees. Below 10 km, the in-air-capturing manoeuvre is performed which requires dedicated simulations as is being investigated in the FALCon project.

The altitude-velocity diagram shows that the B-version is able to reduce its velocity in the higher atmosphere between 50 and 25 km by about 0.4 km/s for the B-version and 0.7 km/s for all others until the horizontal flight phase is achieved. The B-version is also capable of reducing the velocity below 0.5 km/s during the horizontal phase and crosses the sound barrier at about 20 km. The other versions are staying in the supersonic range significantly longer until about 15 km in altitude.

The maximum stagnation point heat flux during the descent occurs slightly before the maximum dynamic pressure due to its correlation with the cube of the velocity in comparison to the square of the velocity for dynamic pressure. It is being calculated by using a modified Chapman approximation equation (see equation 2)

$$\dot{q} = 20254.4 \frac{W}{cm^2} \cdot \sqrt{\frac{\rho}{\rho_r} \cdot \frac{R_{N,r}}{R_N} \cdot \left(\frac{v}{v_r}\right)^{3.05}} \quad (2)$$

With: Reference density  $\rho_r = 1.225 \text{ kg/m}^3$   
 Reference nose radius  $R_{N,r} = 1.0 \text{ m}$   
 Vehicle nose radius  $R_N = 1.0 \text{ m}$  (for all vehicles)  
 Reference velocity  $v_r = 10000 \text{ m/s}$

The B-version has a clear advantage due to its low velocity and low mass peaking at about  $80 \text{ kW/m}^2$ . These values are based on a nose radius of  $1.0 \text{ m}$  for all stages and does not reflect the actual heat flux on the critical parts like the wing’s leading edge. The larger sized G- and MM-stages have a maximum stagnation point heat flux of about  $120 \text{ kW/m}^2$  while the MH-version is at  $100 \text{ kW/m}^2$ . For all stages, the re-entry heat fluxes are significantly higher than during the ascent by a factor of 2.5 and higher.

In contrast, the dynamic pressure for the descent is either approximately equal or even lower than during the ascent which can be attributed to using the wing’s lift to decrease the velocity at as high of an altitude as possible and therefore in a low-density environment. The version B has again the lowest values peaking at about  $25 \text{ kPa}$  both for the ascent and the descent. While the MH-version also has a maximum dynamic pressure of about  $25 \text{ kPa}$  for the descent, the higher power ascent increases this value to over  $40 \text{ kPa}$ , which is considered to be quite high for a launcher with only liquid propulsion and might require throttling in future iterations. The other two versions have peak dynamic pressures between  $30$  and  $40 \text{ kPa}$  for the descent and between  $35$  and  $45 \text{ kPa}$  for the ascent.

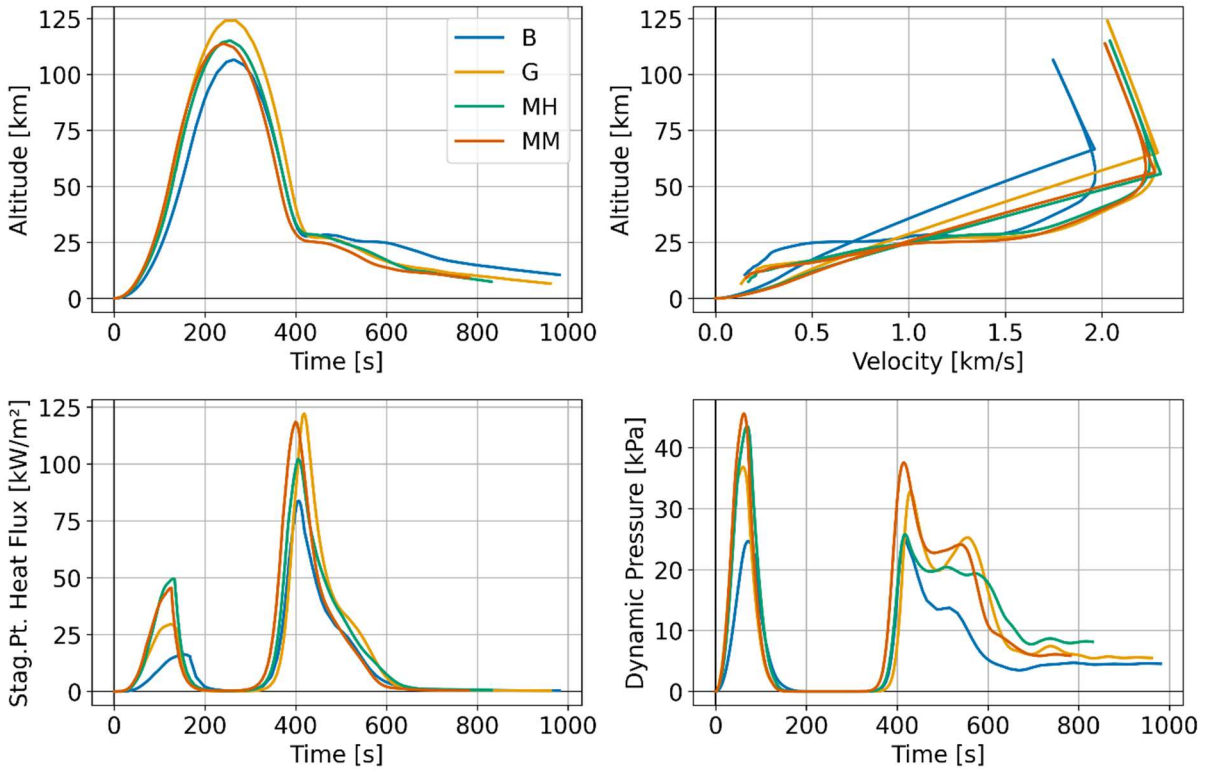


Figure 7: Comparison of the RLV stage’s ascent and decent profile

### 3.7 Discussion

When putting these launchers into the perspective of a European RLV roadmap, they would create the need for a next generation vehicle as the changes are quite large. If the fuel of the second stage is kept at hydrogen and not changed to methane as in the MM-version, it would be the primary part of the vehicle which is still closely designed to the Ariane 6 LLPM. The size of the third stage is about half of the current Ariane 6 ULPM while still keeping the Vinci engine. The fairings are assumed to be the same as for Ariane 6 but have less space in the current design because the third stage is placed within the fairing, which might not be ideal in terms of available space for payloads, especially given the high performance.

The RLV stage is very large and requires substantial development effort, especially in the aerodynamic design of the wing and associated flight dynamics over the whole flight spectrum including ascent, re-entry, in-air-capturing and tow-back. This is projected to require significantly more changes and therefore development budget than what could be required for a vertical landing option. Furthermore, these are projected to cost more in production which makes it financially risky to lose one vehicle and basically rules out the possibility of expending a stage for a high-performance mission.

## 4. Conclusion

During this study, the design of various winged reusable launchers for a future European system has been investigated. With three stages, these are high performance launchers exceeding the current payload target of the Ariane 6 by over 20 percent.

The resulting designs show clear differences between them leading to drastically different designs. From a mass perspective, the hydrolox version with the full-flow staged combustion engine SLME has clear advantages because it reduces the wings size as well as the structural and thermal loads during re-entry. However, this would require a full design cycle of a very challenging engine which could increase the development time substantially.

The clear advantage of the methane versions is that the engines are already in development with Prometheus. However, with both first stages featuring methalox engines, this results in a large and heavy launcher with up to 15 engines in the first stage and 2 in the second stage. Due to its mass, this also creates challenges during re-entry as well as capturing and tow-back.

While the Prometheus-H has only been conceptualized, a similar engine exists in Europe with the Vulcain 2.1. Thus, the delta-development should be achievable. Both from an overall design as well as a mass perspective, the version MH combines the advantages of a small RLV stage with the efficiency of the hydrogen second stage making it an attractive option. However, on the negative side it would require operation and handling of two different propellants as well as not being able to fly “used” RLV engines on the upper stage.

For future studies, these launcher system design need to be expanded and must be investigated in more detail. Furthermore, the design of the wing and its capabilities for re-entry and in-air-capturing must be a focus in the future beyond the predevelopment analysis performed here. All in all, the systems analyzed provide a good starting point for the discussion about the next generation European launchers including a new innovative recoverability method.

## 5. Acknowledgements

Part of this work (booster definition of RLVC4-III-B) was performed within the project ‘Formation flight for in-Air Launcher 1<sup>st</sup> stage Capturing demonstration’ (FALCon) addressing development and testing of the ‘in-air-capturing’ technology. FALCon, coordinated by DLR-SART, is supported by the EU within the Horizon 2020 Programme 5.iii. *Leadership in Enabling and Industrial Technologies – Space* with EC grant 821953. Further information on FALCon can be found at <http://www.FALCon-iac.eu>.

## References

- [1] Sippel, M., Stappert, S., Callsen, S. et al.: *A viable and sustainable European path into space – for cargo and astronauts*, 72<sup>nd</sup> International Astronautical Congress (IAC), Dubai, United Arab Emirates, 2021
- [2] Patureau de Mirand, A., Bahu, J.-M., Gogdet, O.: *Ariane Next, a vision for the next generation of Ariane Launchers*, Acta Astronautica Volume 170 pp. 735-749, 2020
- [3] Sippel, M., et al: *Highly Efficient RLV-Return Mode “In-Air-Capturing” Progressing by Preparation of Subscale Flight Tests*, 8th European Conference for Aeronautics and Space Sciences (EUCASS), Madrid, Spain, 2019
- [4] Sippel, M., Stappert, S., Pastrikakis, V. et al.: *Systematic Studies on Reusable Staged-Combustion Rocket Engine SLME for European Applications*, Space Propulsion Conference, Estoril, Portugal, 2022
- [5] Haeseler, D., Wigger, F., Fortier, Th. et al.: *Vinci® Upper Stage Engine Development, Test, Qualification, and Industrialisation Status for Ariane 6*, 69<sup>th</sup> International Astronautical Congress (IAC), Bremen, Germany, 2018
- [6] Simontacchi, P., Edeline, E., Blasi, E. et al.: *PROMETHEUS: PRECURSOR OF NEW LOW-COST ROCKET ENGINE FAMILY*, 69<sup>th</sup> International Astronautical Congress (IAC), Bremen, Germany, 2018
- [7] Patentschrift (patent specification) DE 101 47 144 C1, *Verfahren zum Bergen einer Stufe eines mehrstufigen Raumtransportsystems*, released 2003
- [8] Krause, S., Cain S.: *UAV Pre-Study for In-Air-Capturing Maneuver*, 2020 IEEE Aerospace Conference, Big Sky Montana, USA, 2020
- [9] Sippel, M., Stappert, S., Bussler, L., Messe, C.: *Powerful & Flexible Future Launchers in 2- or 3-stage Configuration*, 70<sup>th</sup> International Astronautical Congress (IAC), Washington DC, USA, 2019
- [10] Sippel, M., Bussler, L., Krause, S. et al.: *Bringing Highly Efficient RLV-Return Mode „In-Air-Capturing“ to Reality*, 1<sup>st</sup> International Conference on High-Speed Vehicle Science & Technology (HiSST), Moscow, Russia, 2018
- [11] Sippel, M., Stappert, S., Bussler, L. et al.: *Highly Efficient RLV-Return Mode “In-Air-Capturing” Progressing by Preparation of Subscale Flight Tests*, 8<sup>th</sup> European Conference for Aeronautics and Space Sciences (EUCASS), Madrid, Spain, 2019
- [12] Sippel, M., Stappert, S., Singh, S.: *RLV-Return Mode “In-Air-Capturing” and Definition of its Development Roadmap*, 9<sup>th</sup> European Conference for Aeronautics and Space Sciences (EUCASS), Lille, France, 2022
- [13] Singh, S., Bussler, L., Stappert, S. et al.: *Simulation and Analysis of Pull-Up Manoeuvre during In-Air-Capturing of a Reusable Launch Vehicle*, 9<sup>th</sup> European Conference for Aeronautics and Space Sciences (EUCASS), Lille, France, 2022
- [14] Singh, S., Stappert, S., Sippel, M. et al.: *Control Design and Analysis of a Capturing Device performing the In-Air-Capturing of a Reusable Launch Vehicle*, 9<sup>th</sup> European Conference for Aeronautics and Space Sciences (EUCASS), Lille, France, 2022
- [15] Singh, S., Bussler, L., Callsen, S. et al.: *A Superposition Approach to Aerodynamic Modelling of a Capturing Device used for In-Air Capturing of a Reusable Launch Vehicle*, 9<sup>th</sup> European Conference for Aeronautics and Space Sciences (EUCASS), Lille, France, 2022
- [16] Stappert, S., Wilken, J., Bussler, L. et al.: *European Next Reusable Ariane (ENTRAIN): A Multidisciplinary Study on a VTVL and a VTHL Booster Stage*, 70<sup>th</sup> International Astronautical Congress (IAC), Washington D.C., USA, 2019
- [17] Sippel, M., Stappert, S., Bussler, L. et al: *Ultra-Fast Passenger Transport Options Enabled by Reusable Launch Vehicles*, 1<sup>st</sup> International Conference on Flight Vehicles, Aerothermodynamics and Re-Entry Missions & Engineering (FAR), Monopoli, Italy, 2019
- [18] Sippel, M., Stappert, S., Bussler, L. et al: *Technical Progress of Multiple-Mission Reusable Launch Vehicle SpaceLiner*, 1<sup>st</sup> International Conference on High-Speed Vehicle Science & Technology (HiSST), Moscow, Russia, 2018
- [19] Cordesman, A. H., Dawson, V. P.: *Taming Liquid Hydrogen: The Centaur Upper Stage Rocket, 1958 – 2002*, 2004
- [20] ArianeSpace: *Ariane 6 User’s Manual*, Issue 2 Revision 0, 2021
- [21] Stappert, S., Callsen, S., Sippel, M.: *Re-Entry and Flight Dynamics of a Winged Reusable First Stage*, 9<sup>th</sup> European Conference for Aeronautics and Space Sciences (EUCASS), Lille, France, 2022
- [22] Wikimedia Image: *Ariane 62 and 64* [Online]. Available: [https://commons.wikimedia.org/wiki/File:Ariane\\_62\\_and\\_64.svg](https://commons.wikimedia.org/wiki/File:Ariane_62_and_64.svg) [Accessed 19 May 2022]